

Electronic stopping powers of solids for slow atoms

C. M. Kwei,^{1,*} J. J. Chou,¹ J. Yao,¹ and C. J. Tung²

¹*Department of Electronics Engineering, National Chiao Tung University, Hsinchu 300, Taiwan*

²*Department of Nuclear Science, National Tsing Hua University, Hsinchu 300, Taiwan*

(Received 21 February 2001; published 12 September 2001)

Based on the dielectric response theory, electronic stopping powers of solids for slow atoms have been studied. Using a local-field-correction dielectric function, we have calculated these stopping powers by including the correlation and exchange effects. The screening of shellwise electron charge densities of slow atoms by the conduction electrons in solids was estimated using a Thomas-Fermi screening model. In this model, atomic shellwise electron densities were constructed by a superposition of several Yukawa potentials. Stopping powers of Al, Ni, Ag, and Au were calculated for atoms with atomic number between 6 and 18. Calculated results showed that stopping powers oscillated with atomic number consistent with experimental data. Present results also indicated that our approach is much improved over other theoretical calculations. A comparison of presently calculated results with available theoretical and experimental data was made and discussed.

DOI: 10.1103/PhysRevA.64.042901

PACS number(s): 34.50.Bw

INTRODUCTION

Previously, many authors [1–3] calculated the stopping powers of solids for slow atoms based on the dielectric response theory. Brandt and Kitagawa (BK) [1] and Kaneko [2] used the random-phase-approximation (RPA) dielectric function and the extremely-low-velocity approximation in their calculations. Since the RPA dielectric function is valid in the weakly coupled limit of electron correlation, it does not provide accurate information on stopping powers for atoms in a strongly coupled degenerate electron gas system. Wang and Ma (WM) [3] used the local-field-correction (LFC) dielectric function and the low-frequency and long-wavelength approximation. Although the LFC dielectric function includes the exchange and correlation of electrons at short distances from the nucleus, the low-frequency and long-wavelength approximation employed by WM causes errors in stopping powers for slow atoms. In the calculations of BK and WM, the effect of bound electrons in atoms was considered by applying a single Yukawa potential to approximate the electrostatic potential and assuming no screening effect due to conduction electrons in solids. Kaneko estimated the static screening of atomic electrons by conduction electrons in solids using an electron density distribution without detailed shell structures. He found that the screening effect had an influence on the stopping powers of solids for atoms. All authors failed to show the oscillation dependence of stopping powers on the atomic number of atoms.

This paper deals with electronic stopping powers of solids for slow atoms using the LFC dielectric function. However, we incorporate several improvements that include (1) the abandonment of the extremely-low-velocity approximation, (2) the use of atomic shellwise electron density distribution, and (3) the consideration of the screening of the outermost shell electrons by conduction electrons in solids. The atomic shellwise electron densities were constructed by a superpo-

sition of several Yukawa potentials. The screening effect was estimated using a Thomas-Fermi screening model. Stopping powers of Al, Ni, Ag, and Au were calculated for atoms with atomic numbers between 6 and 18. Calculated results showed that stopping powers oscillate with atomic number, consistent with experimental data. Present results also indicated that our approach contains many improvements over other theoretical calculations. A comparison of presently calculated results with available theoretical and experimental data was made and discussed.

THEORY

Within the validity of the linear-response theory, stopping power, $-dE/dx$, of a solid for an atom of atomic number Z_1 is given by [1]

$$-\frac{dE}{dx} = \frac{2}{\pi v^2} \int_0^\infty \frac{dk}{k} |\rho_{ne}(k)|^2 \int_0^{kv} d\omega \omega \operatorname{Im} \left[\frac{-1}{\varepsilon(k, \omega)} \right], \quad (1)$$

where $\varepsilon(k, \omega)$ is the dielectric response function of the solid, k is the momentum transfer, ω is the energy transfer, v is the velocity of the atom, and $\rho_{ne}(\vec{k})$ is the Fourier transform of the charge density of the atom, i.e.,

$$\rho_{ne}(\vec{k}) = \int \rho_{ne}(\vec{r}) e^{-i\vec{k}\cdot\vec{r}} d\vec{r}. \quad (2)$$

Note that all quantities in this work are expressed in atomic units (a.u.) unless otherwise specified. The atomic charge density $\rho_{ne}(\vec{r})$ may be obtained from an electrostatic potential through a Poisson equation given by [4]

$$\rho_{ne}(r) = \sum_i \frac{Z_i}{4\pi r^2} \delta(r) - \sum_i \rho_i(r), \quad (3)$$

where the δ -function term is contributed from the nucleus, $Z_i (i=K, L, M, \dots)$ is the electron occupation number of the

*Author to whom correspondence should be addressed. FAX: (886-3) 5727300. Email address: cmkwei@cc.nctu.edu.tw

i th shell, and the radial electron density distribution of the i th shell corresponding to the superposition of Yukawa potentials may be given by

$$\rho_i(r) = \sum_{j=1}^{n_i} \frac{Z_i}{4\pi r} \alpha_{ij} \beta_{ij}^2 e^{-\beta_{ij} r}. \quad (4)$$

In this work, the parameters α_{ij} and β_{ij} are derived by fitting Eq. (4) to the Hartree-Fock-Slater (HFS) electron density distribution data [5]. For a best fit, we choose $n_i = 2, 3$, and 5 for $i = K, L$, and M shells, respectively. Therefore, the total electron density distribution of the atom may be determined from

$$\rho_e(r) = \sum_i \rho_i(r). \quad (5)$$

Taking the Fourier transform of Eqs. (3) and (4), we obtain

$$\rho_{ne}(k) = \sum_i Z_i - \sum_i \sum_{j=1}^{n_i} Z_i \frac{\alpha_{ij} \beta_{ij}^2}{\beta_{ij}^2 + k^2}. \quad (6)$$

This is the momentum charge density distribution of the atom in free space. For an atom in a solid, conduction electrons of the solid screen the electric field of the atom owing to the dielectric response of the solid. The electron density of the atom is then redistributed. Using a Thomas-Fermi screening model to describe the screening of outermost shell electrons of the atom by conduction electrons of the solid, we obtain the screened charge density as

$$\rho_{ne}^s(r) = \sum_i \frac{Z_i}{4\pi r^2} \delta(r) - \rho_e^s(r), \quad (7)$$

where the screened electron density is given by

$$\begin{aligned} \rho_e^s(r) = & \sum_{i=\text{inner shells}} \sum_{j=1}^{n_i} \frac{Z_i}{4\pi r} \alpha_{ij} \beta_{ij}^2 e^{-\beta_{ij} r} \\ & + \sum_{j=1}^{n_i} \frac{Z_i}{4\pi r} \alpha_{ij} (\beta_{ij} + k_{TF})^2 e^{-(\beta_{ij} + k_{TF})r}. \end{aligned} \quad (8)$$

($i = \text{outermost shell}$)

Here the Thomas-Fermi screen wave number is given by

$$k_{TF} = \left(\frac{4k_F}{\pi} \right)^{1/2} = \frac{1.564}{\sqrt{r_s}}, \quad (9)$$

where k_F denotes the Fermi wave number connected to the number density n of conduction electrons or to the so-called r_s value through

$$k_F = (3\pi^2 n)^{1/3} = \frac{1}{r_s} \left(\frac{9\pi}{4} \right)^{1/3}. \quad (10)$$

Taking the Fourier transform of Eq. (7), we obtain the screened momentum charge density as

$$\begin{aligned} \rho_{ne}^s(k) = & \sum_i Z_i - \sum_{i=\text{inner shells}} \sum_{j=1}^{n_i} Z_i \frac{\alpha_{ij} \beta_{ij}^2}{\beta_{ij}^2 + k^2} \\ & - \sum_{i=1}^{n_i} Z_i \frac{\alpha_{ij} (\beta_{ij} + k_{TF})^2}{(\beta_{ij} + k_{TF})^2 + k^2}. \end{aligned} \quad (11)$$

($i = \text{outermost shell}$)

Thus we replace $\rho_{ne}(k)$ in Eq. (1) by $\rho_{ne}^s(k)$ for stopping power calculations.

To take into account the correlation and exchange effects, we use the LFC dielectric function as given by [6,7]

$$\varepsilon(k, \omega) = 1 - \frac{P(k, \omega)}{1 + G(k)P(k, \omega)}, \quad (12)$$

where $P(k, \omega)$ is the Lindhard polarizability and $G(k)$ is the LFC function to the RPA dielectric function. Introducing the dimensionless variables $q = k/2k_F$ and $u = \omega/(k\nu_F)$, $P(k, \omega)$ can be expressed as

$$P(q, u) = -\frac{\chi^2}{q^2} [f_1(q, u) + if_2(q, u)], \quad (13)$$

where $\chi^2 = 0.166r_s^*$; k_F and ν_F are the Fermi wave number and the Fermi velocity ($k_F = \nu_F$ in atomic units), respectively,

$$f_1(q, u) = \frac{1}{2} + \frac{1 - A_1^2}{8q} \ln \left| \frac{A_1 + 1}{A_1 - 1} \right| + \frac{1 - B_1^2}{8q} \ln \left| \frac{B_1 + 1}{B_1 - 1} \right|; \quad (14)$$

$$f_2(q, u) = \begin{cases} \frac{\pi u}{2}, & B_1 < 1 \\ \frac{\pi}{8q} (1 - A_1^2), & |A_1| < 1 < B_1, \\ 0, & |A_1| > 1; \end{cases} \quad (15)$$

and $A_1 = q - u$ and $B_1 = q + u$. Let $B_1 < 1$ be region I, $|A_1| < 1 < B_1$ be region II and $|A_1| > 1$ be region III. Figure 1 shows the boundaries of regions I, II, and III in the q - u plane. Regions I and II are the single particle-hole excitation regions in which $\text{Im}[-1/\varepsilon(q, u)] \neq 0$. For atoms of low velocity, only single particle-hole excitations contribute to the energy-loss function [8]. The parametrized expression for the LFC function is given by [6,7]

$$\begin{aligned} G(q) = & 16Aq^4 + 4Bq^2 + C + \frac{1 - q^2}{2q} \left[16Aq^4 + 4q^2 \left(B + \frac{8A}{3} \right) \right. \\ & \left. - C \right] \ln \left| \frac{1 + q}{1 - q} \right|, \end{aligned} \quad (16)$$

where $A = 0.029$,

$$B = \frac{9}{16} \gamma_0 - \frac{3}{64} [1 - g(0)] - \frac{16}{15} A, \quad (17)$$

and

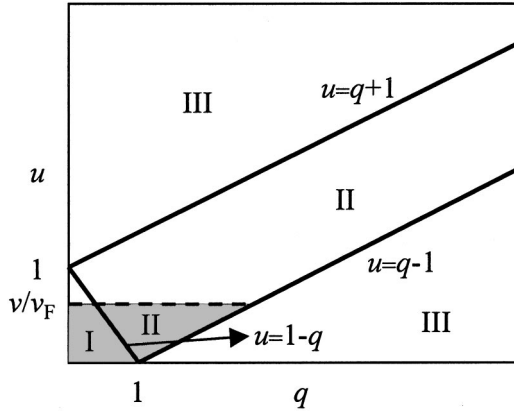


FIG. 1. Boundaries of regions in q - u space. The shadowed region represents the allowed excitation region for slow atoms with velocity ν in the calculation of stopping powers. In this work, we consider values of ν smaller than the Fermi velocity ν_F of the electron-gas system.

$$C = -\frac{3}{4}\gamma_0 + \frac{9}{16}[1 - g(0)] - \frac{16}{5}A. \quad (18)$$

Here $g(0) = (1/8)[z/I_1(z)]^2$ is the radial distribution function at $r=0$, $I_1(z)$ is the first-order modified Bessel function, $z = 4(ar_s/\pi)^{1/2}$, $a = (4/9\pi)^{1/3}$, and γ_0 is connected to the correlation energy of the electron gas $E_c(r_s)$ by

$$\gamma_0 = \frac{1}{4} - \frac{a\pi r_s^5}{24} \frac{d}{dr_s} \left[\frac{1}{r_s^2} \frac{dE_c(r_s)}{dr_s} \right], \quad (19)$$

where

$$r_s \frac{dE_c(r_s)}{dr_s} = \frac{b_0(1 + b_1x)}{1 + b_1x + b_2x^2 + b_3x^3}, \quad (20)$$

$x = \sqrt{r_s}$, $b_0 = 0.0621814$, $b_1 = 9.81379$, $b_2 = 2.82224$, and $b_3 = 0.736411$. For atoms of very low velocity, i.e., $\nu \ll \nu_F$, $f_1(q, u)$, and $f_2(q, u)$ can be further approximated in the long-wavelength limit [8,9].

In terms of the dimensionless variables q and u and substituting $\rho_{ne}^s(k)$ for $\rho_{ne}(k)$, Eq. (1) becomes

$$-\frac{dE}{dx} = \frac{8\nu_F^4}{n\nu^2} \int_0^{\nu/\nu_F} u du \int_0^\infty q |\rho_{ne}^s(2k_Fq)|^2 \text{Im} \left[\frac{-1}{\varepsilon(q, u)} \right] dq. \quad (21)$$

For the case of low velocity atoms with $\nu < \nu_F$, the allowed excitation region is indicated in Fig. 1 as the shadow area. Equation (21) can be rewritten as

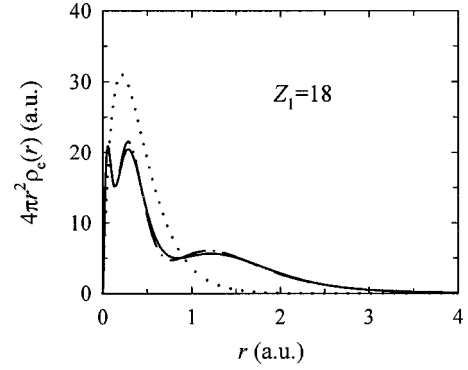


FIG. 2. A plot of the total electron density distribution for an Ar atom as a function of the radial distance from the nucleus. The solid, chain, and dotted curves are results calculated in this work, by the HFS method [5] and by BK [1], respectively.

$$-\frac{dE}{dx} = \frac{8\nu_F^4}{\pi\nu^2} \int_0^{\nu/\nu_F} u du \left\{ \int_0^{1-u} q |\rho_{ne}^s(2k_Fq)|^2 \times \text{Im} \left[\frac{-1}{\varepsilon(q, u)} \right]_I dq + \int_{1-u}^{1+u} q |\rho_{ne}^s(2k_Fq)|^2 \times \text{Im} \left[\frac{-1}{\varepsilon(q, u)} \right]_{II} dq \right\}, \quad (22)$$

where $\text{Im}[-1/\varepsilon(q, u)]_I$ and $\text{Im}[-1/\varepsilon(q, u)]_{II}$ are the energy-loss functions in regions I and II, respectively. In the case of very low-velocity atoms with $\nu \ll \nu_F$, the stopping power reduces to

$$-\frac{dE}{dx} = \frac{8\nu_F^4}{\pi\nu^2} \int_0^{\nu/\nu_F} u du \int_0^1 q |\rho_{ne}^s(2k_Fq)|^2 \text{Im} \left[\frac{-1}{\varepsilon(q, u)} \right]_I dq, \quad (23)$$

which was employed by WM [3], BK [1], and Kaneko [2] with further approximations on ρ_{ne}^s and $\text{Im}[-1/\varepsilon(q, u)]_I$.

RESULTS AND DISCUSSION

Using Eqs. (4) and (5), we have calculated the total electron density distribution for atoms with $6 \leq Z_1 \leq 18$. Figure 2 shows a comparison of this distribution for an Ar atom calculated here (solid curve), by BK (dotted curve), and by the HFS method (chain curve). It is seen that our results are in good agreement with the HFS data. However, the results of BK revealed only an overall structure without detailed shell peaks. Using Eqs. (8) and (9), we calculated the screened electron density distribution for atoms with $6 \leq Z_1 \leq 18$ in Al, Ni, Ag, and Au. Note that we took [10] $r_s = 2.07, 1.6, 1.53$, and 1.49 for Al, Ni, Ag, and Au, respectively. Figure 3 shows a comparison of this distribution for an Ar atom in Al calculated here (solid curve) and by Kaneko (dashed curve). Again, our results reveal shell structures but Kaneko's results do not. A comparison of Figs. 2 and 3 indicates that electron densities with screening effects are larger than those without screening effects at small radial distances. In fact, the screening effect squeezes the outermost electrons to a smaller re-

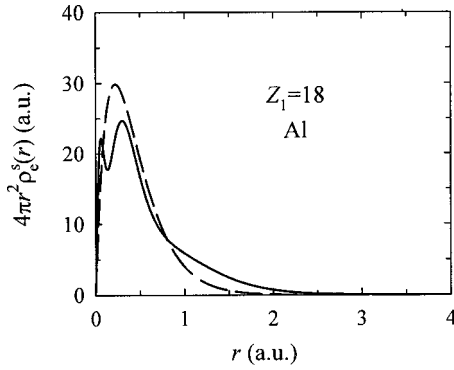


FIG. 3. A plot of the total electron density distribution for an Ar atom screened by conduction electrons in Al as a function of the radial distance from the nucleus. The solid and dashed curves are results calculated in this work and by Kaneko [2], respectively.

gion near the nucleus. In Fig. 4 we plot the momentum charge densities of an Ar atom in free space calculated using Eq. (6) (dashed curve) and the screened momentum charge densities of an Ar atom in Al calculated using Eq. (11) (solid curve). The corresponding results of BK (dotted curve), WM (chain curve) and Kaneko (triangle curve) are also included in this figure for comparisons. The difference between solid and triangle curves or between dashed and dotted curves is due to the effects of shell structures and screening. The results of WM increase rapidly at large- k values due to the long-wavelength approximation used.

Ward *et al.* [11] measured electronic stopping powers of several solids for different atoms with a velocity $\nu = 0.82\nu_0$, where ν_0 is the Bohr velocity. A comparison between calculated results using Eq. (22) (solid circles) and measured data (open circles) is shown in Fig. 5 for different solids. Note that the target-atom mass densities are $\rho_0 = 2.7, 8.89, 10.47,$ and 19.31 g cm^3 for Al, Ni, Ag, and Au, respectively. Other theoretical results plotted in this figure are from WM (dotted curves), Kaneko (dashed curves), and BK (chain curves). Since [10] $\nu_F = 0.9\nu_0, 1.2\nu_0, 1.25\nu_0,$ and $1.28\nu_0$ for Al, Ni, Ag, and Au, respectively, $\nu/\nu_F = 0.9, 0.7, 0.66,$ and 0.64 , correspondingly. Therefore, a neglect of

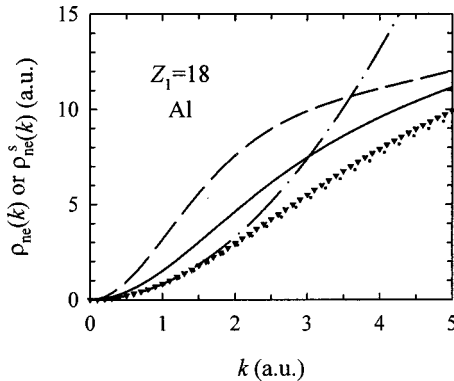


FIG. 4. A plot of the momentum charge density distribution for an Ar atom. The solid, dashed, dotted, chain, and triangular curves are results of present calculations for the screened atom in Al for the unscreened atom in free space, of BK [1], WM [3], and Kaneko [2].

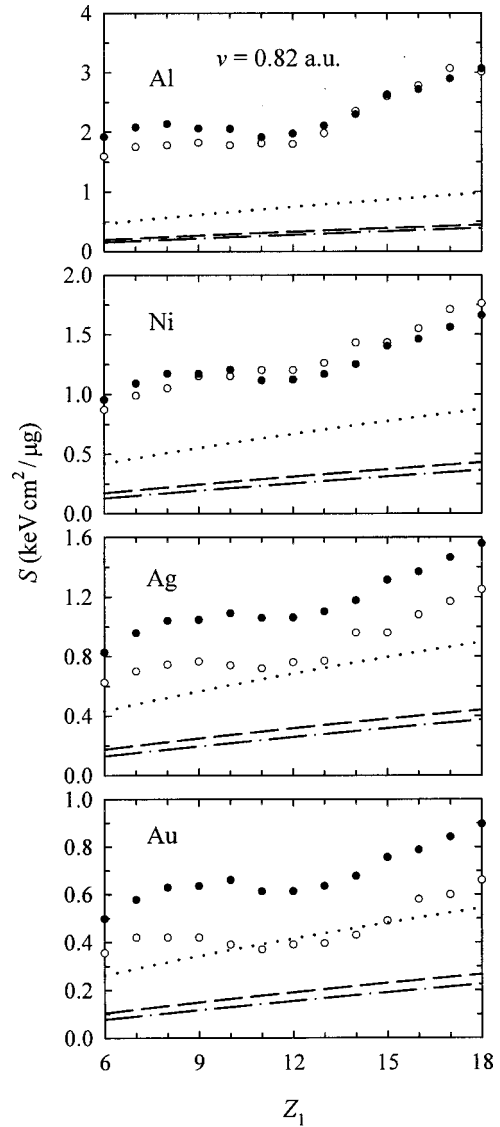


FIG. 5. Electronic stopping cross sections of Al, Ni, Ag, and Au for slow atoms with velocity $\nu = 0.82 \text{ a.u.}$ as a function of atomic number Z_1 . The solid circles, open circles, dotted curves, dashed curves, and chain curves are results of present calculations, experimental data, and results of WM [3], Kaneko [2] and BK [1].

the contribution from region II for allowed excitations by assuming $\nu \ll \nu_F$ by other authors is unreasonable. The present approach, however, includes both contributions from regions I and II for allowed excitations and thus gives results in good agreement with experimental data. It is seen that in all cases present results indicate stopping powers oscillating with atomic number consistent with experimental data. This oscillation behavior is absent in all other calculations. For Ag and Au, present results are somewhat higher than experimental data. This might be due to the use of the Thomas-Fermi screening model and the LFC dielectric function. The LFC dielectric function is derived by a neglect of the frequency dependence of the local-field correction. The static local-field correction is not adequate for solids with complex band structures supporting interband transitions. In such solids, the ion core has a significant effect on conduction electrons

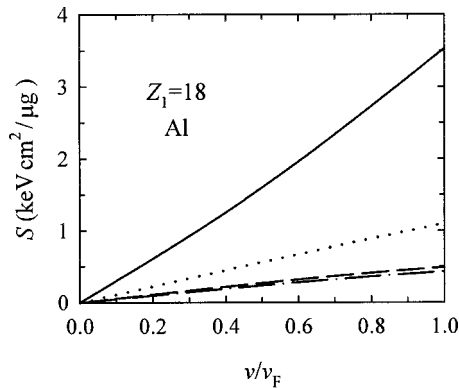


FIG. 6. A comparison of stopping cross sections calculated presently (solid curve), by WM (dotted curve) [3], Kaneko (dashed curve) [2] and BK (chain curve) [1] for an Ar atom in Al as a function of the velocity of the Ar atom.

causing the complexity in energy-loss peaks.

In Fig. 6, we show the velocity dependence of the stopping cross section for an Ar atom in Al. Present results (solid curve) are greater than the results of WA (dotted curve), Kaneko (dashed curve), and BK (chain curve). This is due to the neglect of a contribution from region II for allowed excitations by other authors. Our approach includes both contributions from regions I and II for allowed excitations, and thus gives results in better agreement with experimental data. In all theoretical predications, the stopping cross section increases with velocity of the atom.

CONCLUSIONS

Electronic stopping powers of solids for slow atoms with velocities smaller than the Fermi velocity have been calculated using the LFC dielectric function and the shellwise electron densities screened by conduction electrons in solids. At such velocities, no plasmon excitation contributes to the energy loss, so that only single particle-hole excitations were

considered. Stopping powers of Al, Ni, Ag, and Au were calculated for atoms with an atomic number between 6 and 18. Results exhibited a Z_1 -oscillation dependence in stopping powers, a phenomenon clearly demonstrated by experiments. The present results were in much better agreement with experimental data than other theoretical calculations.

Of the three improvements considered in the present work, an atomic shellwise electron density distribution was responsible for the oscillation of stopping power with projectile charges. The other two improvements, i.e., the abandonment of the extremely low-velocity approximation and the consideration of the screening effect, influenced the magnitude of the stopping power. It could be just a coincidence that the results of WM agreed better in magnitude than present work with experimental data for Ag and Au. As indicated in Eq. (21), the stopping power was proportional to the square of the momentum charge-density distribution. Figure 4 further indicated that the momentum charge-density distribution of WM was unreasonably higher than other theoretical values at large k . In the calculation of the stopping power, however, WM did not include the contribution from region II in Fig. 1. These two effects, one an overestimate and one an underestimate, together made the stopping power of WM in better agreement in magnitude compared with experimental data. As shown in Fig. 4, the momentum charge density distribution without screening effect was higher than with screening effect at all k . Hence the screening effect reduced the stopping power to attain better agreement with experimental data.

For Ag and Au, our results were somewhat higher than the experimental data. This might be due to the use of the Thomas-Fermi screening model and the LFC dielectric function. The LFC dielectric function was derived by a neglect of the frequency dependence of the local-field correction. The static local-field correction was not adequate for Ag and Au, with complex band structures supporting interband transitions. In such solids, the ion core had a significant effect on conduction electrons, causing the complexity in energy-loss peaks.

- [1] W. Brandt and M. Kitagawa, *Phys. Rev. B* **25**, 5631 (1982).
 [2] T. Kaneko, *Phys. Rev. A* **41**, 4889 (1990).
 [3] Y. N. Wang and T. C. Ma, *Phys. Rev. A* **44**, 1768 (1992).
 [4] Y. F. Chen, C. M. Kwei, and C. J. Tung, *J. Phys. B* **26**, 1071 (1993).
 [5] F. Herman and S. Skillman, *Atomic Structure Calculations* (Prentice-Hall, New York, 1963)
 [6] K. Utsumi and S. Ichimaru, *Phys. Rev. A* **26**, 603 (1982).

- [7] Y. N. Wang and T. C. Ma, *Nucl. Instrum. Methods Phys. Res. B* **51**, 216 (1990).
 [8] Y. N. Wang and W. K. Liu, *Phys. Rev. A* **54**, 636 (1996).
 [9] R. H. Ritchie, *Phys. Rev.* **114**, 644 (1959).
 [10] J. F. Ziegler, J. P. Biersack, and U. Littmark, *The Stopping and Range of Ions in Solids* (Pergamon, New York, 1985), p. 264.
 [11] D. Ward *et al.*, *Can. J. Phys.* **57**, 645 (1978).